Acta Cryst. (1997). B53, 113-124

Importance of True Satellite Reflections in the Analysis of Modulated, Composite Crystal Structures. I. A New Refinement of $[M_2Cu_2O_3]_{7+\delta}[CuO_2]_{10}$, $M = Bi_{0.06}Sr_{0.46}Ca_{0.48}$

ANETTE FROST JENSEN,[a]*† FINN KREBS LARSEN,[a] BO BRUMMERSTEDT IVERSEN,[a] VÁCLAV PETŘÍČEK,[b] THOMAS SCHULTZ[a] AND YAN GAO[c]‡

[a]*Department of Chemistry, University of Aarhus, DK-8000 Aarhus C, Denmark,* [b]*Institute of Solid State Physics, Czech Academy of Sciences, Cukrovarnická 10, 162 00 Praha 6, Czech Republic, and* [c]*National Synchrotron Light Source, Brookhaven National Laboratory, Upton, NY 11973, USA. E-mail: frost@xray.ki.ku.dk*

(Received 4 March 1996; accepted 19 September 1996)

Abstract

A new structural model for the composite crystal bismuth strontium calcium cuprate $[M_2Cu_2O_3]_{7+\delta}[CuO_2]_{10}$ with $M = Bi_{0.06}Sr_{0.46}Ca_{0.48}$ and $\delta = 0.03$ has been determined. The structure is orthorhombic with $a = 11.380(2)$, $b = 12.960(4)$ Å and incommensurate along **c**. Sublattice 1 of composition $(CuO_2)_4$ has $c_1 = 2.7522(4)$ Å and sublattice 2 of composition $(M_2Cu_2O_3)_4$ has $c_2 = 3.9155(5)$ Å; superspace group $F222(001+\gamma)001$; modulation vector $\mathbf{q}_1 = \gamma\mathbf{c}_2^*$ with $\gamma = 0.7029(2)$. The structural analysis has been based on 603 main reflections, 428 first-order and 64 second-order satellite reflections. The final residual is $R = 0.0632$ for all reflections, $R = 0.0614$ for main reflections, $R = 0.0735$ for first-order and $R = 0.1084$ for second-order satellite reflections; $\lambda = 0.6565$ Å, $\mu = 19.4$ mm^{-1}. The satellite reflections have been collected with X-ray synchrotron radiation. In this context, special experimental problems are discussed. It is shown that the true satellite reflections, which are the satellite reflections that are not also main reflections for one of the sublattices, are necessary in the least-squares refinement in order to avoid large correlations between displacive modulation amplitudes and thermal vibration amplitudes and thus to obtain a reasonable coordination chemistry.

1. Introduction

The four-dimensional modulated composite structure of $[(Bi,Sr)_{2-x}Ca_xCu_2O_3]_{7+\delta}[CuO_2]_{10}$ with $x \simeq 1.1$ and $\delta = 0.06$ was first published by Kato (1990) based on an analysis of main reflections only. Jensen *et al.* (1993) reported the observation of true satellite reflections for the structure with $x \simeq 1.0$ and $\delta = 0.03$ and published a model refined against 598 main reflections and 66 first-order satellite reflections. The models, however, did not give a satisfactory description of the thermal parameters, due to strong correlations in the least-squares refinement of thermal displacement parameters and modulation displacement parameters. Here we present a new improved model, based on a more extensive and complete data set which, besides 603 main reflections, includes a much larger number of true satellite reflections, 428 first-order and 64 second-order measured with X-ray synchrotron radiation. True satellite reflections are the satellite reflections in a composite structure, which are not main reflections of any of the sublattices. It is shown that inclusion of a large number of satellite reflections leads to chemically more reasonable thermal displacement parameters and interatomic distances, because least-squares correlations between the two types of atomic displacement parameters are drastically reduced. Hitherto, it has not been considered necessary to include true satellite reflections in the refinement of composite structures. Using the formalism derived by Petříček *et al.* (1991) for a description of composite crystal structures, the structure-factor expression for atoms having only harmonic displacements can be written as

$$\begin{aligned} F(hklm) = &\sum_{\nu=1}^{N_1} f_\nu(\mathbf{Q})\exp(2\pi i\mathbf{H}_1.\mathbf{r}_\nu^o) \\ &\times J_m(2\pi\mathbf{H}_1.\mathbf{U}_\nu)(-1)^m\exp(im\varphi_\nu) \\ &+\gamma\sum_{\nu=N_1+1}^{N_2} f_\nu(\mathbf{Q})\exp(2\pi i\mathbf{H}_2.\mathbf{r}_\nu^o) \\ &\times J_l(2\pi\mathbf{H}_2.\mathbf{U}_\nu)(-1)^l\exp(il\varphi_\nu), \end{aligned}$$

where $\mathbf{r}_\nu^o$ is the position of the atom ν in the average structure (sublattice), $\mathbf{U}_\nu$ is a three-dimensional vector describing the modulation amplitude of atom ν, γ is the incommensurate ratio and $f_\nu(\mathbf{Q})$ is the thermally

† Present address: Centre for Crystallographic Studies, Department of Chemistry, University of Copenhagen, Universitetsparken 5, DK-2100 Copenhagen, Denmark.

‡ Present address: Corporate Research and Development, General Electric Company, Schenectady, NY 12301, USA.

averaged scattering factor of atom ν. The first sum is over atoms in sublattice 1 and the second over atoms of sublattice 2. $\mathbf{H}_1 = hkl$, $\mathbf{H}_2 = hkm$, $\mathbf{q} = hklm$, φ_ν is the phase of the modulation, J_m is an mth-order Bessel function, where l and m are the satellite indices. It is evident that each reflection contains information about both sublattices. A main reflection, $hkl0$, $hk0m$, is both a main reflection of one sublattice and a satellite reflection of the other sublattice, while the reflection $hklm$ with all indices nonzero is a pure satellite, mth order of sublattice 1 and lth order of sublattice 2. The structure-factor expression contains two scattering contributions and is not merely a superposition of the scattering of the component lattices.

The orthorhombic composite structure of $[(Bi,Sr)_{2-x}Ca_xCu_2O_3]_{7+\delta}[CuO_2]_{10}$ is a layered structure with two interpenetrating lattices, alternately stacked along the b axis of the unit cell, see Fig. 1. One sublattice is of the composition CuO_2 and consists of edge-sharing CuO_4 squares forming ribbons along the incommensurate direction **c**, while the other sublattice is of the composition $(Bi,Sr)_{2-x}Ca_xCu_2O_3$, a sandwich consisting of a sheet of edge-sharing CuO_4 squares joined in a zigzag pattern along the c axis between layers of presumably statistically distributed Bi, Sr and Ca atoms.

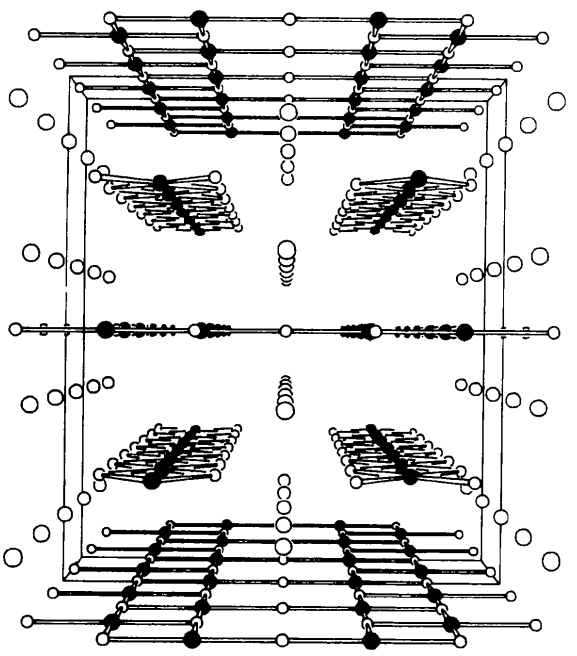

Fig. 1. The composite structure $[(Bi,Sr)_{2-x}Ca_xCu_2O_3]_{7+\delta}[CuO_2]_{10}$. The CuO_2 sublattice consists of the ribbons along **c**, which enter into the picture. The a axis is horizontal, while the b axis, which is the stacking direction, is vertical. The $(Bi,Sr)_{2-x}Ca_xCu_2O_3$ sublattice consists of layers of statistically distributed Bi, Sr and Ca atoms (large circles) and the Cu_2O_3 sheets (top, middle and bottom). Cu atoms are filled circles, O atoms are small circles.

X-ray synchrotron radiation was used to measure the satellite reflections, because they are so weak that collection of a large number is not feasible using a conventional X-ray tube source. The intensity of the strongest satellite reflection only amounts to 5% of the integrated intensity of a strong reflection of the weakest scattering sublattice of composition CuO_2 and to 0.1% of a strong reflection in the common layer of main reflections.

2. Experimental

The synthesis of $[(Bi_{0.06}Sr_{0.46}Ca_{0.48})_2Cu_2O_3]_{7+\delta}[CuO_2]_{10}$ has previously been described in the paper by Jensen *et al.* (1993), which deals with a study of the structure based on diffraction data collected using a Mo X-ray sealed tube source (using $K\alpha$ radiation). Data from that study, which in the following will be termed data set one, have been complemented by X-ray synchrotron radiation data measured using the same single crystal, of size $0.044 \times 0.028 \times 0.240\,mm^3$ along a, b and c, respectively.

X-ray synchrotron data were collected at the X3 beamline at the National Synchrotron Light Source, Brookhaven National Laboratory, USA. The X3A1 station is equipped with a Huber four-circle diffractometer and the synchrotron beam is monochromatized with a Si(111) bent crystal, providing a fixed wavelength of 0.6565 Å. Data were collected with a Bicron Na(I) scintillation counter in ω-step scan mode. The diffractometer control program *ZACK* (Restori & Coppens, 1989) was used.

Because the synchrotron beam is produced by an exponentially decaying electron beam, being replenished at irregular time intervals it is necessary to normalize the measured diffracted intensities. The decay at NSLS was $\sim 50\%$ over 15 h. Variations in the incident intensity were monitored by recording the Compton scattering of a Kapton foil positioned in the beam path. In an attempt to optimize the counts in the monitor to achieve counting statistics better than 1% in each step, the beam defining slits, yielding a beam size of 1.0×1.0 mm at the sample position, were located between the monitor and the sample. This choice later turned out to give some problems in the scaling of the data, because the monitor was not capable of keeping track of small positional variations in the beam, which affected the beam intensity at the sample. Two reflections to be used as reference reflections were remeasured once every hour and when possible just before a beam dump and just after starting data collection with a new beam. In total, 8 d of beam time was used to collect 2184 reflections. Later a third data set was measured at the synchrotron, comprising 1262 data, taking advantage of experience gained with the former data collection. In this case only one intensity control reflection was measured, but every 30 min. Only

reflections which were deemed to have an intensity $I > \sigma(I)$ in the second data collection were measured.

The second and third data set were reduced with a modified version of Blessing's data reduction program package (Blessing, 1987) as follows. The four-indices description of the reflections, necessary for an analysis in a four-dimensional formalism (Petříček *et al.*, 1991), was introduced. The integration mechanism used was a simple trapezoidal procedure. Peak limits were defined for the strong reflections using the minimum $\sigma(I)/I$ criterion (Lehmann & Larsen, 1974), while for weak reflections the outer 1/6 part of the scan in each side was used to create by least-squares fit a linear background which was subtracted from the central 2/3 of the scan defining the peak. Visual inspection of the reflection profiles justified these parameters. E.s.d.'s were calculated by propagation of errors. The polarization correction, $P(\theta) = |\cos 2\theta_m| f_h + (1 - f_h)\cos^2(2\theta)$, was that for a perpendicular geometry, with a once measured degree of horizontal polarization, $f_h = 0.885$ and $|\cos 2\theta_m| = 0.98$, where θ_m is the monochromator Bragg angle.

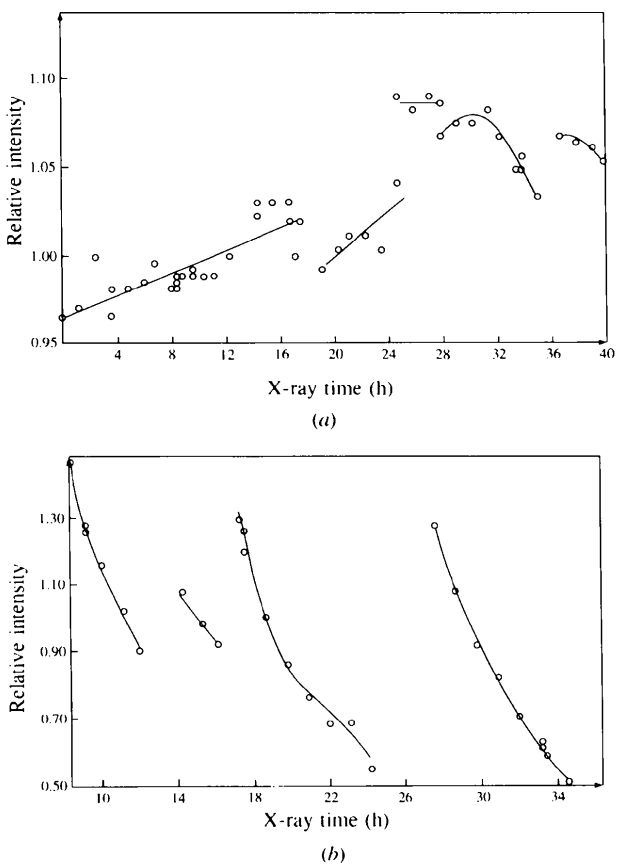

Fig. 2. (*a*) Relative intensity for segments of the standard reflection $2, \bar{1}\bar{4}, 0, 0$ for intensities of data set 2, which have been normalized according to scaling method *A*. The relative intensity scale is from 0.95 to 1.14. The 0's are data points; the curves have been fitted by the *SCALE*3 program (Blessing, 1987). (*b*) Relative intensity of the standard reflection $2, \bar{1}\bar{4}, 0, 0$ for intensities of data set 2 with no normalization to incident counts, as described for scaling method *B*. Intensity scale is from 0.53 to 1.44. The 0's are data points; the curves have been fitted by the *SCALE*3 program (Blessing, 1987).

Two different approaches for scaling were tried: (*a*) A two-step process was applied by first correcting step-by-step the individual detector counts $N_d(n)$ by the corresponding monitor counts $N_m(n)$ according to the formula: $Y(n) = kN_d(n)/N_m(n)$, where k is the same constant for all reflections. Intensities, supposedly free from the effect of beam degradation, were found by integrating $Y(n)$ and then the actual scaling was carried out according to the variation in the intensity of the standard reflections, as is usual in reduction of diffraction data. (*b*) In the other approach no correction for incident intensity variation was applied. Intensities were found by integrating $N_d(n)$ and these were subsequently scaled based on the intensity variation of the standard reflections. Results of the two methods differ little, so for each data set the method which yields the best internal agreement was chosen. It should be remarked that the relative intensities corrected for changing monitor count, very disappointingly for some time segments, had variation of up to 20%, see Fig. 2(*a*) for an example. This variation cannot be attributed to radiation damage of the sample, but may be caused by the experimental setup. The explanation is thought to be that the X-ray beam profile is narrow and much smaller than the beam defining slits. Thus, a shift in beam position due to the instability of the electron beam or thermal fluctuations of the optics of the beamline may cause the most intense part of the beam to be shifted away from the sample position. This will change the count rate at the detector and thus influence $N_d(n)$, while slight beam shifts may not change $N_m(n)$, the Compton scattering at the corresponding time from the Kapton foil, which sits fully irradiated in front of the beam defining slits. Without correction by the monitor count relative intensities of standard reflections were observed to have the expected time structure with generally smooth declines through each fill, as shown in Fig. 2(*b*), although spikes were observed at certain times.

Absorption was corrected for using a numerical method and using the absorption coefficient $\mu = 19.4\ \text{mm}^{-1}$. Since the composition of the cation layer is not accurately known, this absorption correction is only approximate. The data were sorted and averaged using Laue group *mmm*. For satellite reflections the equivalence criterion $I(hklm) = I(\bar{h}klm) = I(h\bar{k}lm) = I(hk\bar{l}\bar{m})$ and equivalence with the Friedel-related reflections were used. Averaging in Laue group 222 was attempted, but the quality of the data did not allow a determination of the handedness of the structure by least-squares refinement and thus results based on *mmm* averaging is reported. This is because the structure is very close to being *mmm* symmetric, except for five satellite reflections. The data from sets 1, 2 and 3 were sorted and averaged with

Table 1. *Synchrotron data collection of satellite reflections from* $[(Bi_{0.06}Sr_{0.46}Ca_{0.48})_2Cu_2O_3]_{7+\delta}[CuO_2]_{10}$

	Data set 2	Data set 3	Data set 4
Scan type	ω	ω	Imaging plate
Number of steps in scan	120	120	
Scan speed (° min^{-1})	0.72	1.00	
Scan width (°)	0.72	0.80	
Monitor counts (s^{-1})	3.0×10^4–1.6×10^5	1.0–1.5×10^4	
Time per step (s)	0.5	0.6	
No. of reflections measured	1684 (satellites) 328 (main)	724 (satellites) 449 (main)	1067 (satellites) 1643 (main)
No. of unique reflections	1189 (satellites) 316 (main)	439 (satellites) 269 (main)	210 (satellites) 327 (main)
No. of observed unique reflections	492 (satellites) 314 (main)	335 (satellites) 253 (main)	107 (satellites) 311 (main)
Internal R value	0.110 (satellites) 0.195 (main)	0.051 (satellites) 0.068 (main)	0.111 (satellites) 0.017 (main)
Data collection period (d)	8	6	1
Standard reflections	2,$\bar{1}$4,0.0, 7910	2,14,0,0	
Time between standards (min)	60	30	
$(\sin\theta/\lambda)_{max}$ (Å^{-1})	0.87	0.64	0.58
Data collection θ range (°)	$0 < \theta < 35$	$0 < \theta < 25$	$0 < \theta < 22$ (not full range)
Data collection range, indices, for single counter data	$hkl\bar{1}$, $l = 2, 3, 4$; $hk1m$, $m = 1, 2, 3, 4$; $hk\bar{1}m$, $m = 1, 2, 3, 4, 5, 6$; $hkl1$, $l = 2, 3, 4$; $hk\bar{2}m$, $m = 2, 3, 4, 5, 6$; $hkl\bar{2}$, $l = 2, 3, 4$; $hk\bar{1}m$, $m = 1, 2, 3, 4, 5, 6$; $(\bar{h}\bar{k}\bar{1}\bar{m})$, $m = 1, 2, 3, 4$. All satellites $h\ 0 \rightarrow 19$, $k\ 0 \rightarrow 22$ $10 < \theta < 40°$; $(hkl0)$, $h\ 0 \rightarrow 21$, $k\ 0 \rightarrow 23, l\ 1 \rightarrow 5$	$hk\bar{1}m$, $m = 1, 2, 3, 4, 5, 6$; $hkl\bar{1}$, $m = 1, 2, 3, 4$; $hk\bar{2}m$, $m = 2, 3, 4, 5, 6, 7$; $hk11$, $hk12$, $hk21$, All satellites $h\ 0 \rightarrow 14, k\ 0 \rightarrow 16$ $10 < \theta < 40°$; $(hkl0)$ $h\ 0 \rightarrow 19$ $k\ 0 \rightarrow 23, l\ 1 \rightarrow 4$	
Wavelength, λ (Å)	0.6565	0.6565	0.6565
Absorption coefficient μ (mm^{-1})	19.4	19.4	19.4
T_{min}, T_{max}	0.24,0.65	0.42, 0.59	0.40, 0.50

an internal agreement of $R_i = 0.038$. Details are given in Table 1 for the synchrotron data and in Jensen *et al.* (1993) for data set 1.

The X3A1 station has now been equipped with an imaging plate area detector system. In this new setup the sample crystal is still mounted on the Huber four-circle diffractometer and the imaging plate is attached to the 2θ arm. 20×25 cm Fuji imaging plates were used and they were read off-line with a Fuji BAS2000 scanner. The data were collected using the oscillation method with a horizontal rotation axis using perpendicular incident beam geometry. Algorithms to treat nonnormal beam incidence for the measurement of high-order reflections have been developed (Bolotovsky, Darovsky, Kezerashvili & Coppens, 1995), but such measurements were not carried out. The crystal-to-detector distance was 123 mm and 10° oscillations were used with 2° overlap between successive plates for scaling purposes, since the incident intensity may vary between different plates. The crystal mosaic spread was 0.25°. A total oscillation range of 138° was recorded. To compensate for the limited dynamic intensity range (10^4) of the imaging plate scanner, the measurements were repeated using an attenuated incident beam. This is particularly important in order to be able to record weak satellite reflections as well as main reflections. The orientation matrices necessary for indexing reflections on the imaging plates were obtained by centering a set of reflections using the scintillation counter and the four-circle diffractometer. The data were integrated with the *HIPPO* program, which employs the seed-skewness method (Bolotovsky, White, Darovsky & Coppens, 1995). Reflections within 1° of the oscillation range limits were discarded. The mosaicity of the crystal was

estimated from ω scans of selected reflections using a scintillation counter.

The data were absorption corrected using a modified version of the program *ABSORB* (DeTitta, 1985). Scaling and averaging in Laue group *mmm* was performed as with data sets 2 and 3. The internal agreement factor ($R_i = 0.017$) for the main reflections of the imaging plate data is much better than found for the previous data sets, while for the satellite reflections the internal agreement ($R_i = 0.111$) is inferior to that of data set 3. These satellite reflections of data set 4 were consequently discarded. The better internal agreement factor for the main reflections is attributed to the fact that the influence of beam instabilities at the sample position can be considerably reduced by oscillation over the range several times and by scaling on intensity of symmetry-equivalent reflections. The internal agreement for the main reflections is comparable to that obtained by Bolotovsky, Darovsky, Kezerashvili & Coppens (1995) for the strong reflections in a charge density study of $Cr(NH_3)_6Cr(CN)_6$. Similarly, the agreement factor for the satellite reflections is comparable to the values obtained for weak high-order reflections in that study. Details of data collection and reduction are listed in Table 1.

The final set of data was chosen as the merge of data sets 1–4, although the satellite reflections of set 4 were not used. In total, the merged data set, on which the refinement was based, comprises 1372 unique main reflections {of which 603 were considered observed [$I > 3\sigma(I)$]}, 976 unique first-order (428 observed) and 297 unique second-order satellite reflections (64 observed).

3. Results

3.1. *Superspace symmetry*

The composite structure consists of two sublattices with composition CuO_2 and $M_2Cu_2O_3$, where $M = Bi_{0.06}Sr_{0.46}Ca_{0.48}$ is a mixed-metal layer. The diffraction pattern can be fully indexed using four indices, *hklm*. Sublattice 1, which is the CuO_2 lattice, has main reflections *hkl*0, while sublattice 2 ($M_2Cu_2O_3$) has main reflections *hk*0*m*. The plane *hk*00 is common, which means that $\mathbf{a}_1^* = \mathbf{a}_2^* = \mathbf{a}^*$ and $\mathbf{b}_1^* = \mathbf{b}_2^* = \mathbf{b}^*$, but $\mathbf{c}_1^* \neq \mathbf{c}_2^*$. For this case, $\mathbf{c}_1^* = \gamma\mathbf{c}_2^*$, where $\gamma = c_1/c_2 = 0.7029$. True satellite reflections are described by *hklm*, $l \neq 0$, $m \neq 0$. The systematic extinction conditions of the reflections, which are for all *hklm*: $h + k = 2n$, $h + l + m = 2n$ and $k + l + m = 2n$, yield the Bravais class $mmmF(001 + \gamma)$. The superspace description is based on the formalism developed by Janner & Janssen (1980) and de Wolff, Janner & Janssen (1981).

The composite structure is close to centrosymmetric. It may be centrosymmetrically described in the origin-shifted superspace group $Fmmm(001 + \gamma)ss1$ with the symmetry operations as follows and basis ($\mathbf{a}$, $\mathbf{b}$, $\mathbf{c}_1 - \gamma\mathbf{e}_4$, $\mathbf{e}_4$), where $\mathbf{e}_4$ is a vector in internal space perpendicular to physical space

(1)	x_1	x_2	x_3	x_4
(2)	$\frac{1}{2} - x_1$	x_2	x_3	$\frac{1}{2} + x_4$
(3)	x_1	$-x_2$	x_3	$\frac{1}{2} + x_4$
(4)	$\frac{1}{2} + x_1$	x_2	$-x_3$	$-x_4$
(5)	$-x_1$	$-x_2$	$-x_3$	$-x_4$
(6)	$\frac{1}{2} + x_1$	$-x_2$	$-x_3$	$\frac{1}{2} - x_4$
(7)	$-x_1$	x_2	$-x_3$	$\frac{1}{2} - x_4$
(8)	$\frac{1}{2} - x_1$	$-x_2$	x_3	x_4

and centering translations (0,0,0,0), (1/2,1/2,0,0), (0,1/2,1/2,1/2) and (1/2,0,1/2,1/2). The $\mathbf{q}$ vector $\mathbf{q}_1 = \gamma\mathbf{c}_1^*$, where $\gamma = 0.7029$ has been used for indexing the reflections, and not $\mathbf{q}_1 = (\gamma + 1)\mathbf{c}_1^*$. $\mathbf{r}'' = (x_1, x_2, x_3)$ is the average atomic position in sublattice 1, while $x_4 = \mathbf{q}_1.\mathbf{r}'' = \gamma x_3 + t$. t is a coordinate in the internal space and t also expresses the noninteger part of the projection of sublattice 2 onto sublattice 1. It varies between 0 and 1. This nomenclature was also applied in the previous study of the same structure (Jensen *et al.*, 1993).

However, the observation of five first-order satellite reflections, $02\bar{1}\bar{1}$, $0,12,1,\bar{5}$, $0,12,1,\bar{1}$, $0,12,1,3$ and 8013, which all have $3\sigma(I) < I < 10\sigma(I)$, suggests the superspace group to be noncentrosymmetric $F222(001 + \gamma)001$, which retains the four symmetry operations (1), (6), (7) and (8) with the centering translations. These five satellite reflections violate the extinction rules

$$(h0lm)\ l = 2n, m = 2n \text{ and } (0klm)\ l = 2n, m = 2n,$$

which arise from the presence of glides in the centrosymmetric superspace group. The two superspace groups have the same atomic positions, but there is a difference in the number of modulation amplitudes allowed. For the centrosymmetric superspace group only half as many are allowed as for the noncentrosymmetric one. Since these questionable reflections are weak, refinements in both superspace groups were performed and a statistical R-factor test (Hamilton, 1965; Pawley, 1970) was used to help determine the superspace group. For main reflections the agreement indices were very similar and a centrosymmetric model could not be excluded. For satellite reflections, however, there were significant differences in the R factor and use of the statistical R-factor tests allowed the rejection of the centrosymmetric group at the 0.1% error level. These tests were performed on a set of data where the five forbidden reflections in $Fmmm(001 + \gamma)ss1$ were excluded, together with three other first-order satellites, which were very badly fitted [$\Delta F/\sigma(F) > 10$] in this superspace group. Therefore, the noncentrosymmetric superspace group was chosen. This superspace group is the same as was used in the paper by Kato (1990) and by Jensen *et al.* (1993), but in a different setting. In the latter publication the superspace group was named $P{:}F222{:}\bar{1}\bar{1}1$. The present

Table 2. *Refinement A*

Parameters from the composite refinement *A*.

(*a*) x, y, z are fractional atomic coordinates. Displacement parameters u_{ij} are given in Å^2. U_i^s is the modulation amplitude of the sine wave and U_i^c is that of the cosine wave. Modulation amplitudes are given in Å. Cu3 and O3 belong to sublattice 1, Cu1, O1, O2 and *M* to sublattice 2.

	Cu1	O1	O2	*M**	Cu3	O3
Occupation	1/2	1/2	1/4	1/2	1/4	1/2
x	0.33421 (6)	0.1686 (4)	1/2	1/2	1/4	0.1367 (3)
y	1/4	1/4	1/4	0.38015 (6)	1/2	1/2
z	1/4	1/4	1/4	3/4	1/4	3/4
u_{11}	0.0027 (3)	0.0047 (16)	0.002 (2)	0.0090 (3)	0.0048 (4)	0.0104 (14)
u_{22}	0.0200 (4)	0.022 (2)	0.031 (4)	0.0114 (4)	0.0162 (5)	0.0229 (17)
u_{33}	0.0007 (4)	0.0007 (18)	0.006 (3)	0.0086 (4)	0.0301 (8)	0.027 (3)
u_{12}	0	0	0	0	0	0
u_{13}	0	0	0	−0.0012 (10)	0	0
u_{23}	0.0 (0)	0.0 (0)	0	0	0	−0.021 (3)
U_x^s (q)	0	0	0	−0.0459 (6)	0	0
U_y^s (q)	−0.0548 (7)	−0.073 (4)	0	0	0	0.311 (6)
U_z^s (q)	0.0088 (16)	−0.021 (9)	−0.037 (13)	−0.0013 (16)	0	−0.026 (14)
U_x^c (q)	0.04 (2)	0.011 (10)	0	0	0	−0.004 (11)
U_y^c (q)	0	0	0	0.0073 (17)	0	0
U_z^c (q)	0	0	0	0	0.029 (4)	0
U_x^s (2q)	0	0	0	−0.009 (4)	0	0
U_y^s (2q)	−0.001 (4)	−0.03 (2)	0	0	0	0.038 (11)
U_z^s (2q)	−0.0040 (7)	0.001 (4)	−0.010 (7)	0.0296 (8)	−0.0236 (15)	−0.068 (7)
U_x^c (2q)	0.0044 (11)	0.008 (7)	0	0	0	0.035 (4)
U_y^c (2q)	0	0	0	0.0001 (14)	0	0
U_z^c (2q)	0	0	0	0	0	0

(*b*) Modulation of thermal vibration parameters for the *M* atoms in Å^2.

ij	11	22	33	12	13	23
$u_{ij,1}^s$				0.00010 (15)		0.0019 (4)
$u_{ij,1}^c$	−0.0027 (7)	0.0015 (6)	0.0038 (6)		−0.00260 (13)	
$u_{ij,2}^s$				−0.0016 (8)		0.0006 (4)
$u_{ij,2}^c$	−0.0004 (4)	−0.0018 (4)	0.0010 (3)		−0.0000 (10)	

* Occupancy of Bi: 0.06(0), occupancy of Sr: 0.460 (10), occupancy of Ca: 0.480 (10).

setting allows us to compare directly the structure with that of $[(Bi_{0.04}Sr_{0.96})_2Cu_2O_3]_7[CuO_2]_{10}$ described in part II of this paper (Jensen, Petříček, Larsen & McCarron, 1997).

3.2. *Structural chemistry*

The refinements were carried out with the program *JANA*94 (Petříček, 1994) using 1095 observed [$I > 3\sigma(I)$] reflections comprising 603 main reflections, 428 first-order and 64 second-order satellite reflections.

The atomic position of atom number ν in sublattice i in a modulated composite crystal has been described as

$$\mathbf{r}_{\nu i} = \mathbf{r}^o_{\nu i} + \sum_{k=1}^{2} \mathbf{U}^s_{\nu,k}\sin(2\pi k\mathbf{q}_i.\mathbf{r}^o_{\nu i}) + \mathbf{U}^c_{\nu,k}\cos(2\pi k\mathbf{q}_i.\mathbf{r}^o_{\nu i}),$$

where $\mathbf{r}^o_{\nu i}$ is the position of the atom in the average structure (sublattice), k is the order of the harmonic, $\mathbf{U}^s_\nu$ and $\mathbf{U}^c_\nu$ are three-dimensional vectors describing the modulation amplitudes, and $\mathbf{q}_i$ is the modulation vector for sublattice i. $\mathbf{U}^s_\nu$ and $\mathbf{U}^c_\nu$ have to obey symmetry restrictions for atoms on special positions. These restrictions are automatically implemented by *JANA*94 according to the given superspace symmetry. Similarly, modulation of thermal parameters has been described as follows

$$u_{ij} = u^o_{ij} + \sum_{k=1}^{2} u^s_{ij,k}\sin(2\pi k\mathbf{q}_i.\mathbf{r}^o_{\nu i}) + u^c_{ij,k}\cos(2\pi k\mathbf{q}_i.\mathbf{r}^o_{\nu i}),$$

where u^o_{ij} is the thermal parameter of the given atom.

The atomic parameters from this refinement are listed in Table 2(*a*). $\mathbf{r}^o_{\nu i} = (x, y, z)$ of the sublattices are given, together with $\mathbf{U}^s_\nu$ and $\mathbf{U}^c_\nu$. Refinements showed that only *M* atoms have significant modulation of thermal parameters and so in refinement *A* only *M* atoms were supplied with this type of parameter, see Table 2(*b*). Two other refinements on subsets of the data have been performed, refinement *B* including just a few satellite reflections and refinement *C* including no satellite reflections at all. The refined model is slightly different, since in refinements *B* and *C* no modulation of thermal parameters was included. *R* factors for different classes of reflections are given in Table 3, together with a listing of the charac-

Table 3. *Different refinement models and their agreement values*

	Refinement *A*	Refinement *B*	Refinement *C*
Second-order displacive modulation harmonics	Yes	Yes	Yes
Temperature factor modulation	Yes	No	No
Number of nonpositive definite displacement ellipsoids	0	2	4
No. of correlation coefficients, $\rho_{ij} > 0.7$.	0	7	17
Max shift/e.s.d.	0.002	0.022	0.003
No. of main reflections	603	598	598
No. of first-order satellite reflections	428	66	0
No. of second-order satellite reflections	64	0	0
Goodness-of-fit	1.52	1.83	1.82
No. of parameters	67	54	54
R, wR, all reflections	0.0632, 0.0645	0.0623, 0.0666	0.0607, 0.0643
R, wR, main reflections	0.0614, 0.0568	0.0623, 0.0666	0.0607, 0.0643
R, wR, first-order satellite reflections	0.0735, 0.090	0.0655, 0.0654	—
R, wR, second-order satellite reflections	0.1084, 0.1308	—	—

$R = \sum ||F_o| - |F_c|| / \sum |F_o|$. $wR = [\sum w(F_o^2 - F_c^2)]^{1/2} / [\sum wF_o^2]^{1/2}$. Weight $w = (\sigma_{cts}^2 + 0.0004F^2)^{-1}$.

teristics of the different refinements. Parameters corresponding to refinements *B* and *C* have been deposited.*

The composition for the mixed cation site *M* has been refined to $Bi_{0.06}Sr_{0.46}Ca_{0.48}$. The Bi content was fixed to that of an X-ray fluorescence analysis (Jensen *et al.*, 1993) and the occupancy of Sr and Ca was refined, constraining the sum of occupations to the *M* site occupancy. The composition derived from the refinement deviates slightly from that found in the X-ray fluorescence analysis, which was $Bi_{0.06}Sr_{0.39}Ca_{0.55}$. Parameters describing the occupational (substitutional) modulation of Sr and Ca were not statistically significant and therefore they were eliminated from the model. It has been suggested (Aracheeva & Shamrai, 1994) that Bi does not reside on the Sr/Ca site, but on the Cu sites. This postulate was based on a supercell refinement. We have tested the hypothesis by refining an occupancy of Bi on the Cu sites constraining the sum of the Cu and Bi occupations to the site occupancy. For both the Cu1 and Cu3 sites, the Bi occupancies refined to a nonsignificant negative number, numerically less than 1% of the Cu occupation. We therefore are led to the conclusion that it is not likely that either of the Cu sites are partly occupied by Bi. In the Bi–Sr–Ca–Cu oxide superconductors to which this compound is structurally related, Bi has been reported to occupy up to 6% of the (separate) Sr and Ca sites (Lee *et al.*, 1989), as for the present compound. The BiO layers in the superconductors have a distorted rock salt structure with Bi in octahedral coordination. The coordination chemistry of Sr/Ca in the present compound is more similar to that of BiO layers than that of the distorted square-planar Cu oxide environment. From the above we conclude that Bi, Sr and Ca are statistically distributed over the same atomic site.

* Lists of atomic coordinates, anisotropic displacement parameters, complete geometry and structure factors, and a Fourier map diagram have been deposited with the IUCr (Reference: SH0077). Copies may be obtained through The Managing Editor, International Union of Crystallography, 5 Abbey Square, Chester CH1 2HU, England.

4. Discussion

For the least-squares refinements against sets of data with only a limited number of true satellite reflections (refinements *B* and *C*), large correlations between thermal vibration displacement parameters and modulation displacement parameters occurred (Table 3). These correlations have been completely eliminated in refinement *A*, where all correlation coefficients are below 0.7.

4.1. *Thermal vibration*

The description of the thermal vibration is poor in refinement *C*, but slightly better in refinement *B* where fewer negative u_{ii} appear. Only in refinement *A*, however, the description of the thermal vibration appears to be satisfactory, with all atoms having positive definite displacement ellipsoids. u_{33} for Cu1 and O1 are still quite small, possibly due to insufficiencies in the absorption correction. The thermal displacement parameters in refinement *A* can be considered physically reasonable, since for each of the three structural components in the layer structure, the Cu_2O_3 sheets, the CuO_2 ribbons and the *M* layer, the atoms of the component have the same shape of the vibrational ellipsoids. For Cu_2O_3 the mean-square displacements out of the sheet plane along **b** are at least an order of magnitude larger than the in-plane displacements (**a**, **c**), while for CuO_2 both mean-square displacements in the stacking direction **b** and along the incommensurate direction **c** are several times larger than displacements along **a**. The large displacement along **c** can probably be ascribed to disorder in the structure. Electron diffraction images of the compound (with slightly different compositions of the cation layer *M*) show that reflections of the CuO_2 sublattice are streaked in a direction perpendicular to **c*** (Wu, Takayama-Muromachi, Suehara & Horiuchi, 1991; Milat, van Tendeloo, Amelinckx, Mehbod & Deltour, 1992). Wu *et al.* interpret this to be due to a phase shift of neighboring CuO_2 ribbons, which

they consider displaced as rigid bodies. Our imaging plate recordings similarly showed the CuO_2 sublattice diffraction spots with extended diffuse streaks perpendicular to **c***. This effect was even more pronounced for $[(Bi_{0.04}Sr_{0.96})_2Cu_2O_3]_7[CuO_2]_{10}$, described in part II (Jensen, Petříček, Larsen & McCarron, 1997). This disorder cannot be modeled by displacive modulation.

This model differs from previously published models in that modulations of thermal vibration amplitudes for the *M* site have been included. The introduction of this modulation had a profound influence on the agreement indices for the satellite reflections, which decreased from 12.4 to 7.3% for first-order and from 14.0 to 10.9% for second-order satellite reflections. The largest amplitude amounts to 50% of the corresponding thermal vibration (u_{33}). The main reflections were not affected by the thermal vibration parameter modulation. The modulation of thermal parameters had no significant influence on the displacive modulation for the *M* site and no impact at all on the thermal displacement or displacive modulation parameters for the Cu and O atoms. It is therefore not the reason for the differences in interatomic distances between refinement *A* and those of refinements *B* and *C*. The physical explanation for the modulation of the thermal vibration is that the coordination of the atom changes with t because of positional (displacive) modulation. This makes the interatomic potential a function of t and therefore also the atomic thermal motion. This modulation was suggested from a difference-Fourier map in the x_3x_4 plane calculated with *JANA*94 before inclusion of thermal parameter modulation in the model (Fig. 3*a*). Up to 1 e Å^{-3} peaks are observed in the map, which disappear on introduction of thermal parameter modulation (Fig. 3*b*). A Fourier map of the x_3x_4 section has been deposited.* Thermal vibration parameter modulation for the Cu atoms was not statistically significant and thus not included in the final model.

* See deposition footnote on p. 119.

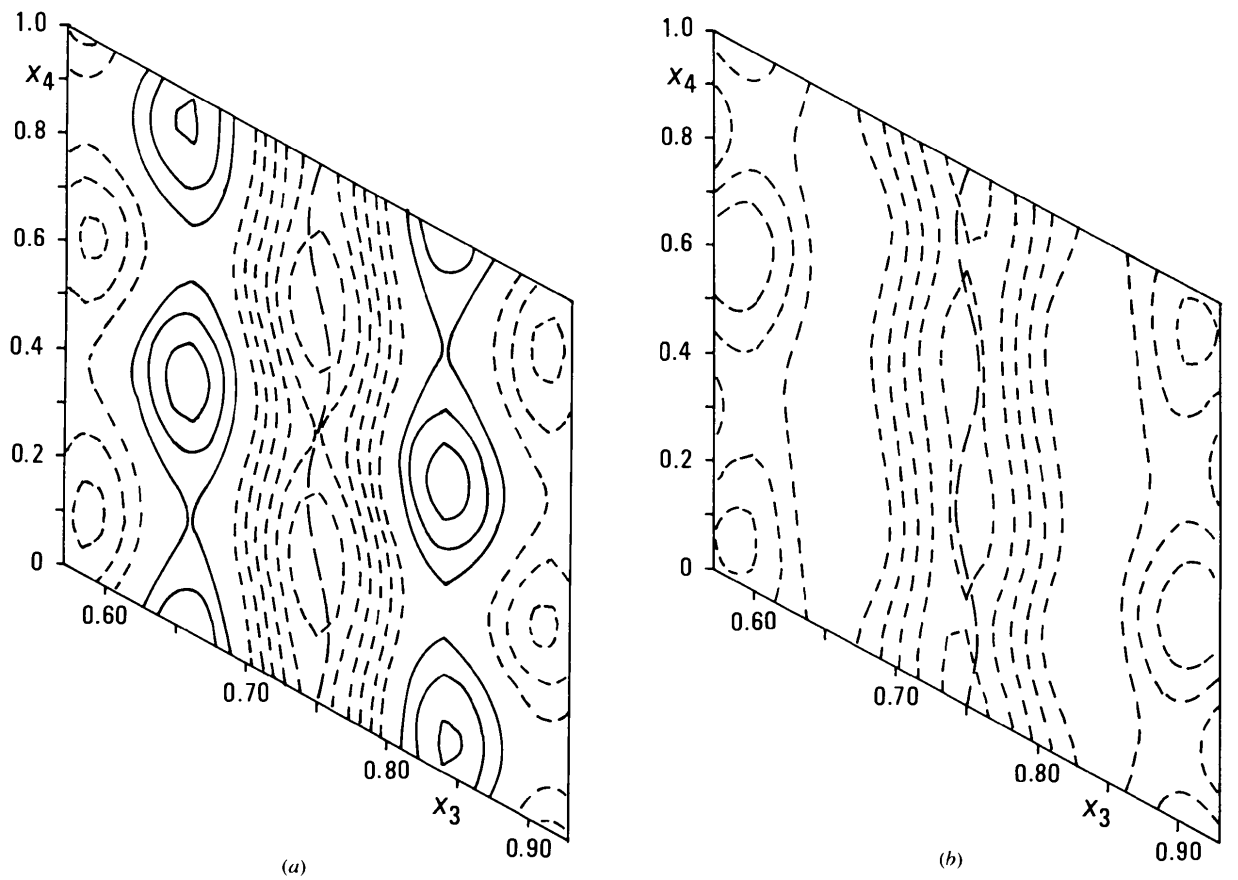

Fig. 3. (*a*) Difference-Fourier map, showing the trace (long dashed line) in the (x_3,x_4) plane of the *M* site before inclusion of thermal parameter modulation in the refined model. Large peaks of the remaining electron density are observed. Positive electron density is represented by full lines, negative density by short dashed lines. The contour level is 0.3 e Å^{-3}. (*b*) Difference-Fourier map, showing the trace in the (x_3,x_4) plane of the *M* site after inclusion of thermal parameter modulation in the refined model. The remaining electron density lobes from (*a*) are seen to have disappeared. Contours as for (*a*).

4.2. *Interatomic distances*

The most important difference between this refinement *A* and those hitherto published lies in the description of the displacive modulation amplitudes. On inclusion of more satellite reflections, the e.s.d.'s have decreased, but the displacive modulation amplitudes have also become significantly smaller. This has led to substantial changes in the interatomic distances. Results are shown in Table 4 for refinement *A* and have been deposited for refinements *B* and *C*.* The interatomic distances have been calculated with the program *TDIST* (Císařová, 1991). Cu3 is coordinated to four O3 atoms with distances in the range 1.826 (10)–1.979 (11) Å, while Cu1, coordinated to three O1 atoms and one O2 atom, have distances ranging from 1.873 (13) to 1.989 (9) Å. These ranges are significantly smaller than previously reported. Kato (1990) reported Cu3 to oxygen distances of 1.785 (16)–2.000 (18) Å and Cu1 to oxygen distances of 1.770 (14)–2.144 (18) Å. This may also be compared with the results of Jensen *et al.* (1993), who had at their disposal only a limited set of first-order satellites. After correction for an erroneous scale factor, the ranges of interatomic distances in their case, here termed refinement *B*, are for Cu3 to oxygen 1.83 (2)–1.96 (2) Å and for Cu1 to oxygen 1.75 (2)–2.15 (2) Å. Finally, refinement *C*, refined on 598 main reflections only, gave Cu3 to oxygen distances of 1.73 (5)–2.19 (4) Å and Cu1 to oxygen distances of 1.73 (3)–2.25 (3) Å. The same trend is evident for the *M* to oxygen distances.

In Figs. 4(*a*)–(*c*) to 7(*a*)–(*c*) the interatomic distances have been mapped as a function of the internal coordinate *t* for refinements *A*, *B* and *C*. Distances are repeated with the periodicity of the reciprocal modulation vector for the sublattice, *i.e.* c_2 for atoms of sublattice 1. Therefore, central atoms of sublattice 1 (Cu3, O3) have distance periodicity 1 in *t*, while central atoms of sublattice 2 (*M*, Cu1, O1, O2) have distance periodicity $\gamma = 0.7029$ in *t*. Figs. 4(*a*)–(*c*) show Cu3 to O3 distances. There are in total four distances, which are pairwise identical. Refinements *A* and *B* have very similar curves, while refinement *C* shows a very large variation. The inclusion of even very few true satellite reflections thus has a profound influence on the interatomic distances. Figs. 5(*a*)–(*c*) show Cu1 to O1 and O2 distances. For refinement *A*, there is little variation as a function of *t*. The two lower curves correspond to distances along **a** (O1 and O2), the upper two to distances along **c**. The variation in distances along **c** (Cu1—O1) for both refinements *B* and *C* are (unrealistically) huge. The shortest contact Cu1—O3 is 2.896 (7) Å for refinement *A* and has not been depicted, since it is not considered bonding. *M* is coordinated to four O atoms (O1 and O2) in the same sublattice and to two or three others (O3) in the other sublattice. The intralattice distances

Table 4. *Interatomic distances: refinement A*

	Minimum (Å)	Maximum (Å)	Average (Å)
$Cu1^{i}—O1^{i}$	1.873 (13)	1.891 (8)	1.853 (12)
$Cu^{i}—O1^{ii}$	1.938 (9)	1.989 (9)	1.9595 (9)
$Cu1^{i}—O1^{iii}$	1.938 (9)	1.989 (9)	1.9595 (9)
$Cu1^{i}—O2^{i}$	1.879 (2)	1.893 (10)	1.8870 (2)
$Cu3^{i}—O3^{i}$	1.826 (10)	1.979 (11)	1.8990 (11)
$Cu3^{i}—O3^{iv}$	1.826 (10)	1.979 (11)	1.8992 (10)
$Cu3^{i}—O3^{v}$	1.826 (10)	1.979 (11)	1.8992 (10)
$Cu3^{i}—O3^{vi}$	1.826 (10)	1.979 (11)	1.8990 (11)
$M^{i}—O1^{ii}$	2.519 (15)	2.596 (17)	2.5553 (15)
$M^{i}—O1^{vii}$	2.519 (15)	2.596 (17)	2.5553 (15)
$M^{i}—O2^{i}$	2.537 (10)	2.620 (9)	2.5847 (9)
$M^{i}—O2^{viii}$	2.537 (10)	2.620 (9)	2.5847 (9)
$M^{i}—O3^{vii}$	2.400 (11)	3.933 (9)*	
$M^{i}—O3^{ix}$	2.396 (10)	2.643 (11)*	
$M^{i}—O3^{x}$	2.396 (11)	3.070 (12)*	
$M^{i}—O3^{xi}$	2.409 (8)	4.295 (13)*	

*Maximum value in the interval $0 < t < 0.70$, the distance goes towards infinity outside this interval in *t*. Symmetry codes: (i) x_1, x_2, x_3, x_4; (ii) $\frac{1}{2} - x_1, \frac{1}{2} - x_2, \frac{1}{2} + x_3, \frac{1}{2} + x_4$; (iii) $\frac{1}{2} - x_1, \frac{1}{2} - x_2, x_3 - \frac{1}{2}, x_4 - \frac{1}{2}$; (iv) $\frac{1}{2} - x_1, x_2, \frac{1}{2} - x_3, -x_4$; (v) $x_1, x_2, x_3 - 1, x_4 - 1$; (vi) $\frac{1}{2} - x_1, 1 - x_2, x_3, x_4$; (vii) $\frac{1}{2} + x_1, x_2, \frac{1}{2} + x_3, \frac{1}{2} + x_4$; (viii) $x_1, x_2, x_3, 1 + x_4$; (ix) $\frac{1}{2} - x_1, 1 - x_2, x_3, x_4$; (x) $\frac{1}{2} + x_1, x_2, x_3 - \frac{1}{2}, \frac{1}{2} + x_4$; (xi) $\frac{1}{2} - x_1, 1 - x_2, x_3 - 1, x_4$.

from *M* to O1 and O2 are shown in Figs. 6(*a*)–(*c*). The *M*—O1 bond is along **a**, while the *M*—O2 bond is along **c**. The *M*—O2 bond is reasonably well described in both refinements *A* and *B*, while only refinement *A* describes the *M*—O1 bond well. The minimum distance *M*—O1 is severely affected by lowering the number of satellite reflections in the refinement and it decreases from 2.519 (15) to 2.40 (3) Å from refinement *A* to *B*. When comparing with Figs. 7(*a*)–(*c*), which show the interlattice distances *M*—O3, we see that for values of *t*, where intralattice distances are short, there are only two short interlattice distances, while for long intralattice distances, there are three short interlattice distances. The minimal distance is larger in refinement *A*. It is evident that only refinement *A* gives a reasonable coordination chemistry for all atoms and that a large number of true satellite reflections are needed in the refinement to avoid correlations between the different types of atomic displacement parameters, namely the thermal vibration amplitudes and the displacive modulation amplitudes. For this type of structure it may not be sufficient to have at one's disposal only good main reflections for the composite refinement. This is evident from the structural model published by Kato (1990), which on the basis of only main reflections refines to $R = 0.028$ and still shows a significantly negative u_{11} for O1 and very large interatomic distances for Cu1 to O atoms.

5. Conclusions

It has been shown that for the structure $[(Bi,Sr)_{2-x}Ca_xCu_2O_3]_{7+\delta}[CuO_2]_{10}$, inclusion of true

* See deposition footnote on p. 119.

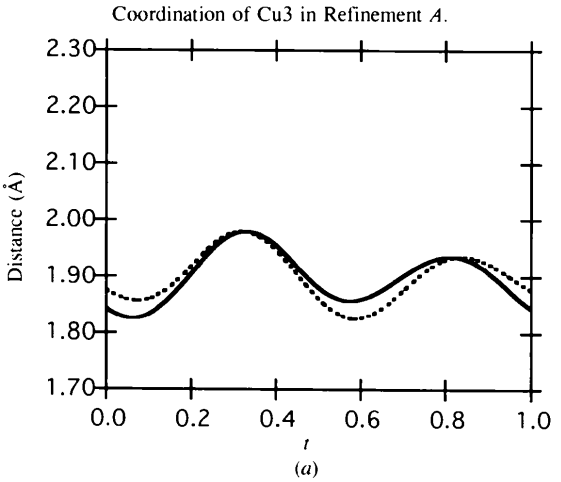

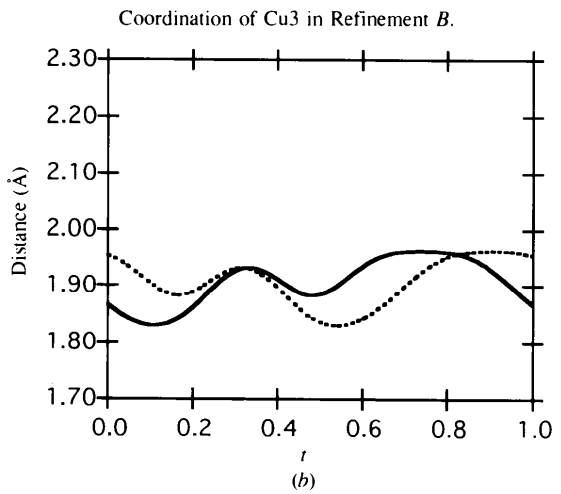

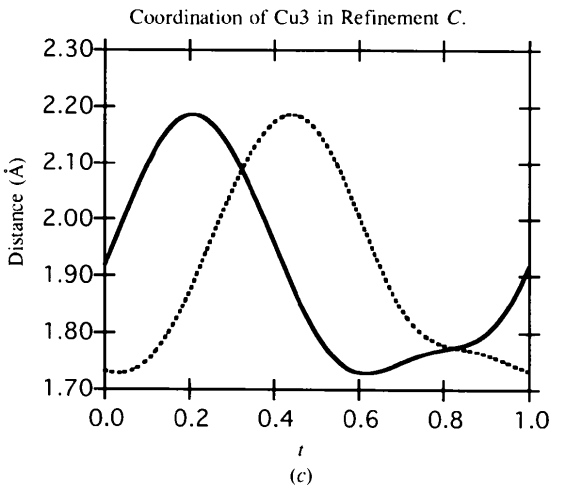

Fig. 4. (*a*)–(*c*). The interatomic distances as a function of t, mapped for the Cu3—O3 distances in sublattice 1. Two distances (to O3 atoms with equal x_3 coordinate) have the same value at any t. In total, four Cu3—O3 bonds exist. The local coordination is obtained for one given value of t. (*a*) is for refinement *A*, (*b*) for refinement *B* and (*c*) for refinement *C*.

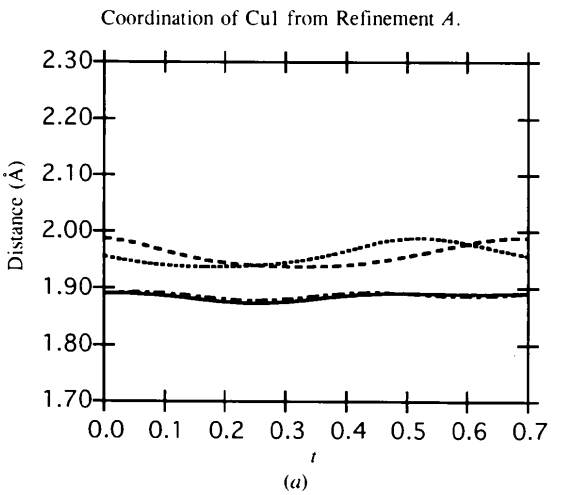

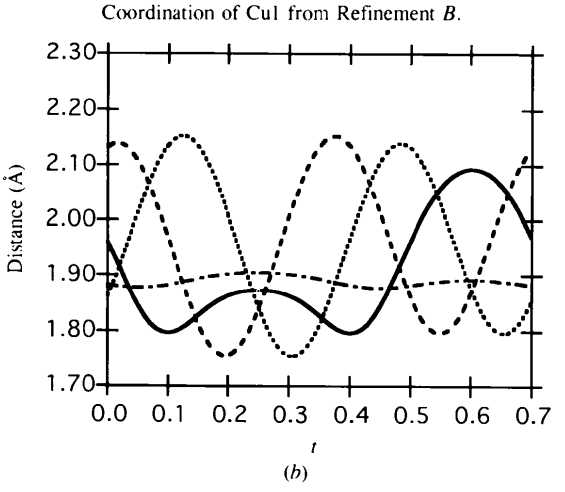

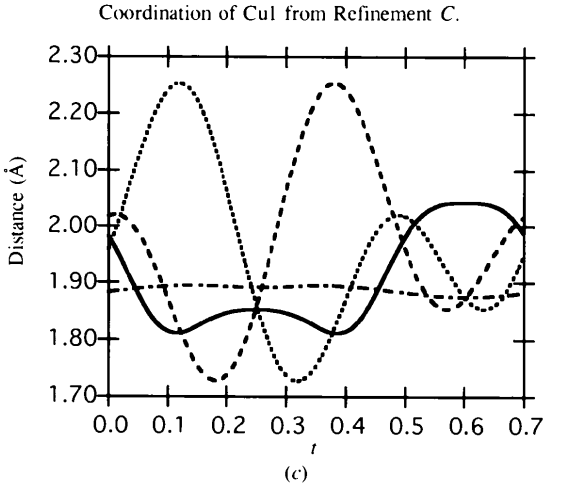

Fig. 5. (*a*)–(*c*). The interatomic distances as a function of t, mapped for the Cu1—O1 and Cu1—O2 distances in sublattice 2. (*a*) is for refinement *A*, (*b*) for refinement *B* and (*c*) for refinement *C*. The two upper curves in (*a*) correspond to distances along **c**, while in (*b*) and (*c*) these distances are represented by the curves with the largest variations. The two lower curves in (*a*) are distances along **a** (those with least variation in *b* and *c*).

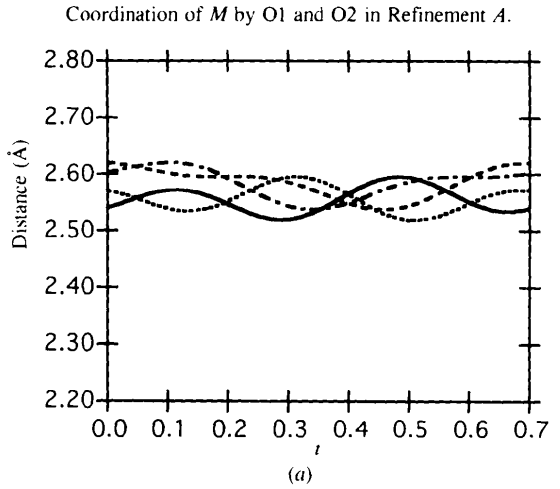

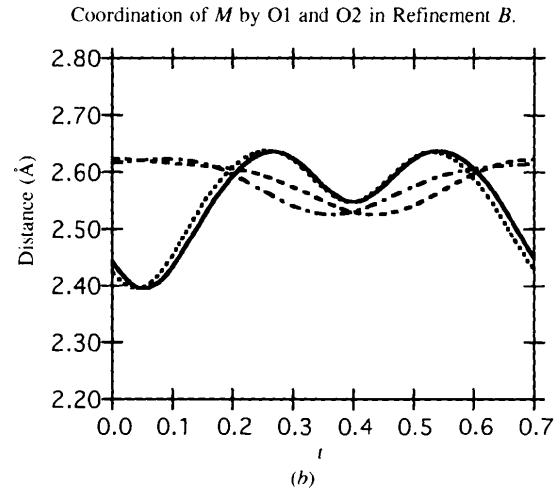

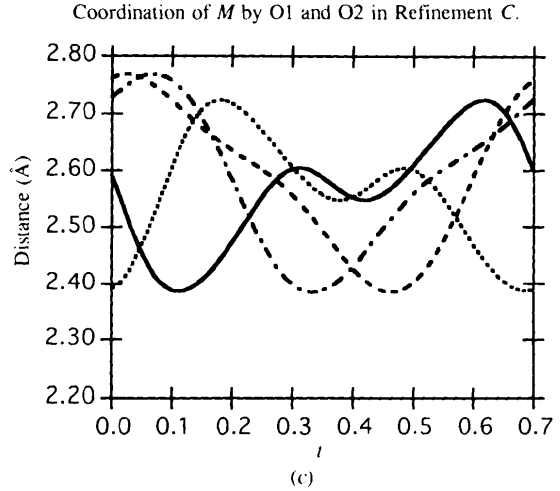

Fig. 6. (*a*)–(*c*). The interatomic distances as a function of *t*, mapped for the *M*—O1 and *M*—O2 intralattice distances in sublattice 2. The two upper curves at $t = 0$ correspond to *M*—O2 distances, while the two lower ones correspond to *M*—O1 distances. (*a*) is for refinement *A*, (*b*) for refinement *B* and (*c*) for refinement *C*.

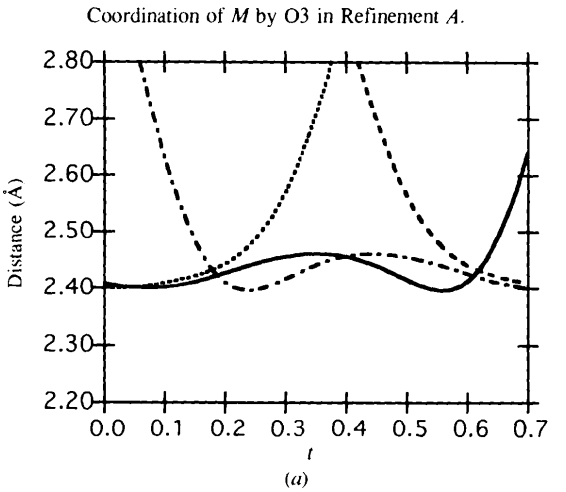

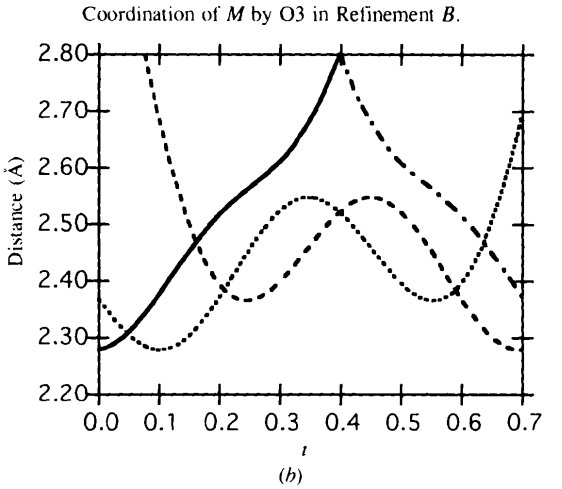

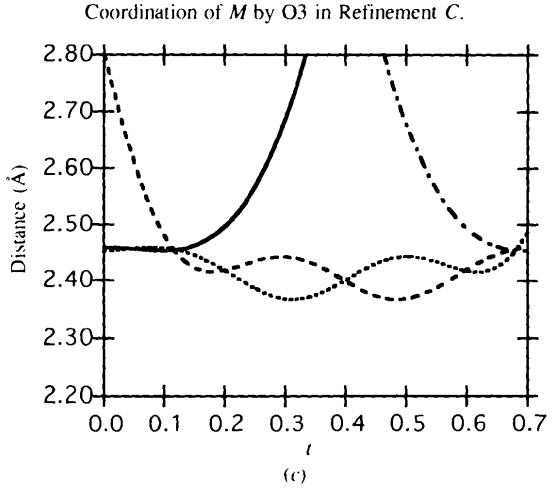

Fig. 7. (*a*)–(*c*). The interatomic distances as a function of *t*, mapped for the *M*—O3 interlattice distances. (*a*) is for refinement *A*, (*b*) for refinement *B* and (*c*) for refinement *C*.

satellite reflections in the least-squares refinement is necessary to obtain a chemically sound structural model.

It is not obvious that it should be so. Several composite structures have been refined on main reflections only with good results. Examples are the misfit layer compounds $(MS)_xTS_2$, where M = Sn, Pb, Bi or lanthanide elements and T = Ti, V, Cr, Nb, Ta, and $1.08 < x < 1.23$ (Wiegers & Meershaut, 1992, and references therein). These compounds all have extremely weak true satellite reflections if any. True satellite reflections have been observed by X-ray diffraction only for $(LaS)_{1.14}NbS_2$, $(PbS)_{1.18}TiS_2$ and $(LaS)_{1.20}CrS_2$ (van Smaalen, 1992). Whereas $(LaS)_{1.14}NbS_2$ was refined on both main and true satellite reflections (van Smaalen, 1991), the remaining two compounds were refined on main reflections only (van Smaalen, Meetsma, Wiegers & de Boer, 1991; Kato, 1990). For $(PbS)_{1.18}TiS_2$ satellites were later measured and shown to fit well into the structural model (van Smaalen, 1992).

For other modulated composite structures, such as the organic conductors $(BEDO\text{-}TTF)_{2.4}I_3$ (Ciśařová *et al.*, 1991) and $(BEDT\text{-}TTF)Hg_{0.776}(SCN)_2$ (Wang *et al.*, 1991), the displacive modulations are so large that the true satellites are easily observable with conventional X-ray radiation and they are therefore readily included in the refinement.

On the basis of the present work, we may advise that if the refined structural model of a modulated composite structure shows chemically or physically unreasonable parameters, true satellite reflections should be measured and included in the refinement.

The United States Department of Energy is gratefully acknowledged for granting us beamtime at the National Synchrotron Light Source at beamline X3. It is a pleasure to thank Dr Alex Darovsky, the State University of New York, beamline X3, for assisting us with the data collections at the beamline. We are indebted to the Carlsberg Foundation for the low-temperature Huber diffractometer in Aarhus. The Danish Natural Science Research Council is gratefully acknowledged for Ph.D. fellowships to AFJ and BBI, and a travel grant to FKL. AFJ wishes to acknowledge a post-doctoral fellowship from the Human Capital and Mobility program of the European Union. VP acknowledges a grant from the Grant Agency of the Czech Republic.

References

Aracheeva, A. V. & Shamrai, V. F. (1994). *Sov. Phys. Crystallogr.* **38**, 40–51. (In Russian.)

Blessing, R. H. (1987). *Cryst. Rev.* **1**, 3–58.

Bolotovsky, R., Darovsky, A., Kezerashvili, V. & Coppens, P. (1995). *J. Synchrotron Rad.* **2**, 181–184.

Bolotovsky, R., White, M., Darovsky, A. & Coppens, P. (1995). *J. Appl. Cryst.* **28**, 86–95.

Císařová, I. (1991). *TDIST. A Program for Calculation of Distances in a Modulated, Composite Structure.* State University of New York at Buffalo, Buffalo, NY, USA.

Císařová, I., Maly, K., Bu, X., Jensen, A. F., Sommer-Larsen, P. & Coppens, P. (1991). *Chem. Mater.* **3**, 647–651.

DeTitta, G. T. (1985). *J. Appl. Cryst.* **18**, 75–79.

Hamilton, W. C. (1965). *Acta Cryst.* **18**, 502–510.

Janner, A. & Janssen, T. (1980). *Acta Cryst.* A**36**, 408–415.

Jensen, A. F., Larsen, F. K., Johannsen, I., Císařová, I., Maly, K. & Coppens, P. (1993). *Acta Chem. Scand.* **47**, 1179–1189.

Jensen, A. F., Petříček, V., Larsen, F. K. & McCarron, E. M. (1997). *Acta Cryst.* B**53**, *XXX–XXX*(SH0079).

Kato, K. (1990). *Acta Cryst.* B**46**, 39–44.

Lee, P., Gao, Y., Sheu, H.-S., Petříček, V., Restori, R., Coppens, P., Darovsky, A., Phillips, J. C., Sleight, A. W. & Subramanian, M. A. (1989). *Science*, **244**, 62–63.

Lehmann, M. S. & Larsen, F. K. (1974). *Acta Cryst.* A**30**, 580–584.

Milat, O., van Tendeloo, G., Amelinckx, S., Mehbod, M. & Deltour, R. (1992). *Acta Cryst.* A**48**, 618–625.

Pawley, G. S. (1970). *Acta Cryst.* A**26**, 691–692.

Petříček, V. (1994). *JANA*94. *Programs for Modulated and Composite Crystals.* Institute of Physics, Czech Academy of Sciences, Praha, Czech Republic.

Petříček, V., Maly, K., Coppens, P., Bu, X., Císařová, I. & Jensen, A. F. (1991). *Acta Cryst.* A**47**, 210–216.

Restori, R. & Coppens, P. (1989). *ZACK. A Program for Collection of Single Crystal Data in Four-Circle Geometry, Including Options for Treatment of Higher Dimensional Crystals, Synchrotron Radiation and Electric Field Experiments.* State University of New York at Buffalo, Buffalo, NY, USA.

Smaalen, S. van (1991). *J. Phys. Condens. Matter*, **3**, 1247–1263.

Smaalen, S. van (1992). *Incommensurate Sandwiched Layered Compounds. Materials Science Forum*, edited by A. Meerschaut, Vols. 100 and 101, pp. 173–222. Zurich: Trans. Tech. Publications, Ltd.

Smaalen, S., van, Meetsma, A., Wiegers, G. & de Boer, J. L. (1991). *Acta Cryst.* B**47**, 314–325.

Wang, H. H., Beno, M. A., Carlson, D., Thorup, N., Murray, A., Porter, L. C., Williams, J. M., Maly, K., Bu, X., Petříček, V., Císařová, I., Coppens, P., Jung, D., Whangbo, M.-H., Schirber, J. E. & Overmyer, D. L. (1991). *Chem. Mater.* **3**, 508–513.

Wiegers, G. A. & Meerschaut, A. (1992). *Incommensurate Sandwiched Layered Compounds. Materials Science Forum*, edited by A. Meerschaut, Vols. 100 and 101, pp. 101–172. Zurich: Trans. Tech. Publications, Ltd.

Wolff, P. M. de, Janner, A. & Janssen, T. (1981). *Acta Cryst.* A**37**, 625–636.

Wu, X.-J., Takayama-Muromachi, E., Suehara, S. & Horiuchi, S. (1991). *Acta Cryst.* A**47**, 727–735.